Inorganic Chemistry

Article

pubs.acs.org/IC

A 3D Iron(II)-Based MOF with Squashed Cuboctahedral Nanoscopic Cages Showing Spin-Canted Long-Range Antiferromagnetic Ordering

Soumyabrata Goswami, Amit Adhikary, Himanshu Sekhar Jena, Soumava Biswas, and Sanjit Konar*

Department of Chemistry, IISER Bhopal, Bhopal-462023, India

Supporting Information

ABSTRACT: The reaction of dilithium squarate with Fe(II) perchlorate led to the formation of a new Fe(II)-based 3D MOF, $[Fe_3(OH)_3(C_4O_4)(C_4O_4)_{0.5}]_n$ (**1**), with homoleptic squashed cuboctahedral cages. Complex **1** crystallizes in the monoclinic *C*2/*c* space group. Fe(II) centers in the complex are octahedrally coordinated by four squarate dianions in axial and equatorial positions and two hydroxyl groups in the remaining equatorial positions. The interesting structural feature of **1** is that the three-dimensional framework is an infinite extension of nanoscopic cuboctahedral cages. The framework also contains two types of voids; the larger hydrophobic ones are surrounded by aromatic squarate ligands, while the smaller ones are hydrophilic with hydroxyl groups on the surface connected by bifurcated hydrogen bonding interaction. A variable temperature magnetic study shows spin-canted long-range antiferromagnetic ordering in the low temperature regime.

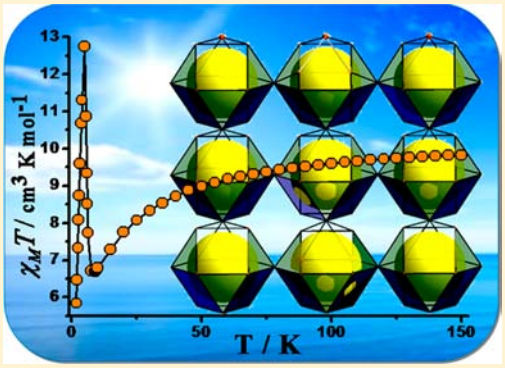

INTRODUCTION

Self-assembled polyhedral structures are common in biology and now also in chemistry, thanks to the advancement of supramolecular chemistry. The preparation of discrete polyhedral molecular assemblies having regular geometry is still a synthetic challenge. Over the past few years, syntheses of cuboctahedral nanoscopic cages have been reported by a few groups[1] but are all zero dimensional. Higher dimensional molecules formed by aesthetically appealing high-symmetry polyhedral units are rare and immensely interesting.[2,3] In this context, the fabrication of Metal Organic Frameworks (MOF), a novel class of functional organic−inorganic hybrid materials, incorporating nanoscopic polyhedral morphologies is a newly emerging field of research. Moreover, these higher dimensional frameworks formed by squashed nanoscopic coordination cages have attracted great attention, as they offer the possible synergism of different features,[4] the most important being the tempting high symmetry polyhedral structures like tetrahedra, truncated tetrahedra, capped truncated tetrahedra, cuboctahedra, etc.[1a,b] though their structures in many cases arise serendipitously. Besides structural beauties, MOFs are also known for their potential applications in drug delivery, gas storage, luminescence, and molecular magnetism.[5−8] But the creation of porous magnets or Magnetic Metal Organic Frameworks (MMOFs)[6] is a long-sought academic goal since in MOFs the connection between paramagnetic metal centers at distances within interacting range can be obtained by proper designing of ligands rendering the material magnetic. Here, we have chosen the squarate dianion $(C_4O_4)^{2-}$ as the ligand[9−11] because it has versatile coordination modes (Scheme S1) and could mediate strong magnetic interactions among the metal centers. It also has a high electron density aromatic core which could form electron-rich pore surfaces and therefore should have good affinity and selectivity for electron-accepting molecules. Our present report deals with the magnetic as well as gas-sorption property studies of a 3D Fe(II) framework, $[Fe_3(OH)_3(C_4O_4)(C_4O_4)_{0.5}]_n$ (**1**), formed of nanoscopic cuboctahedral cages. The detailed magnetic studies reveal spin-canted long-range antiferromagnetic ordering in the low temperature region, and gas adsorption studies show selectivity toward CO_2 and CH_4 adsorptions over N_2.

EXPERIMENTAL SECTION

Materials and General Procedure. All the reagents and solvents were commercially available and were used as obtained. Squaric acid, lithium carbonate, and $Fe(ClO_4)_2{\cdot}6H_2O$ were obtained from the Sigma Aldrich Chemical Co. Dilithium squarate was prepared by dissolving lithium carbonate and squaric acid in water in a 1:1 molar ratio, stirring for a few hours, and finally evaporating the solvent to get a white colored solid compound.

Caution! *Perchlorate salts are potentially hazardous, and caution should be exercised when dealing with such salts.*

The elemental analyses were carried out on Elementar Microvario Cube Elemental Analyzer. FT-IR spectra (4000−400 cm^{-1}) were recorded on KBr pellets with a Perkin-Elmer Spectrum BX spectrometer. Powder X-ray diffraction (PXRD) data were collected on a PANalytical EMPYREAN instrument using Cu Kα radiation. N_2, CO_2, and CH_4 adsorption studies were performed using a BELSORP

Received: July 22, 2013
Published: October 1, 2013

   dx.doi.org/10.1021/ic401886f | *Inorg. Chem.* 2013, 52, 12064−12069

MAX (BEL Inc., Japan) volumetric adsorption analyzer. Magnetic measurements were performed using a Quantum Design VSM SQUID magnetometer. The measured values were corrected for the experimentally measured contribution of the sample holder, while the derived susceptibilities were corrected for the diamagnetism of the samples, estimated from Pascal's tables.[12]

Synthesis of $[Fe_3(OH)_3(C_4O_4)(C_4O_4)_{0.5}]_n$ (1). Li-squarate (0.4 mmol, 50 mg) was taken in 20 mL of water and stirred for 10 min to dissolve completely. $Fe(ClO_4)_2{\cdot}6H_2O$ (0.2 mmol, 50 mg) was dissolved in 20 mL of acetonitrile, and 2 mL of this Fe(II) solution was slowly and carefully layered with 2 mL of the above aqueous solution, using 1 mL of a 1:1 mixture of water and acetonitrile as a third middle layer to slow down the diffusion, in a narrow glass tube. Cube-shaped crystals were formed after few weeks in the tube. The crystals were separated, washed with cold water and Et_2O, and air-dried (yield 58%). Anal. Calcd for $C_{12}H_6Fe_3O_{18}$: C, 23.1; H, 0.98%. Found: C, 23.79; H 1.01%. FT-IR (KBr pellet, 4000−400 cm^{-1}): ν(O−H) 3433 cm^{-1} and ν(C−C and C−O) 1521 cm^{-1} (Figure S1).

Crystal Data Collection and Structure Determination. A yellowish brown cube-shaped crystal of **1** was chosen for X-ray structural analysis, and intensity data were collected on a Brüker APEX-II CCD diffractometer using a graphite monochromated Mo Kα radiation source (α = 0.71073 Å) at 296 K. Data collection was performed using φ and ω scans. The structures were solved using direct methods followed by full matrix least-squares refinements against F^2 (all data HKLF 4 format) using SHELXTL.[13] A multiscan absorption correction, based on equivalent reflections, was applied to the data. Anisotropic refinement was used for all non-hydrogen atoms. Hydrogen atoms were placed in appropriate calculated positions. Crystallographic data for **1** are summarized in Table 1.

RESULTS AND DISCUSSION

Crystal Structure of $[Fe_3(OH)_3(C_4O_4)(C_4O_4)_{0.5}]_n$ (1). Complex **1** crystallized in the monoclinic space group $C2/c$.

Table 1. X-Ray Crystallographic Data and Refinement Parameters for 1

	1
formula	$C_{12}H_6Fe_3O_{18}$
M_w (g mol^{-1})	605.72
cryst size (mm)	0.38 × 0.34 × 0.32
cryst syst	monoclinic
space group	$C2/c$
T (K)	296
a (Å)	11.5656(11)
b (Å)	11.5662(11)
c (Å)	16.346(2)
α (deg)	90.00
β (deg)	90.444(3)
γ (deg)	90.00
V (Å^3)	2186.5(4)
Z	4
ρ_{calcd} (g cm^{-3})	1.840
μ(Mo Kα) (mm^{-1})	2.048
F(000)	1200.0
T_{max}, T_{min}	0.519, 0.464
h, k, l range	$-17 \le h \le 17$, $-17 \le k \le 17$, $-24 \le l \le 21$
collected reflns	3933
independent reflns	2811
goodness-of-fit (GOF) on F^2	1.151
R1, wR2 ($I > 2\sigma I$)[a]	0.0902,0.2458
R1, wR2 (all data)[a]	0.0945, 0.2488
CCDC number	931819

[a] $R1 = \sum||F_o| - |F_c||/\sum|F_o|$. $wR2 = |\sum w(|F_o|^2 - |F_c|^2)|/\sum|w(F_o)^2|^{1/2}$.

The relevant bond parameters around the Fe(II) centers are listed in Table 2. The Fe(II) centers in the complex have

Table 2. Bond Distances (Å) and Bond Angles (deg) around Fe(II) Found in 1

bond lengths (Å)		bond angles (deg)	
Fe1 − O1	2.127(2)	O1− Fe1 − O7	94.7(2)
Fe1 − O7	2.092(3)	O2−Fe2 − O5	86.2(2)
Fe2 − O2	2.130(3)	O2− Fe2− O8	84.5(2)
Fe2 − O5	2.128(2)	O5− Fe2− O8	84.6(2)
Fe2 − O8	2.087(2)	O6− Fe3− O9	85.7(2)
Fe3 − O6	2.122(2)		
Fe3 − O9	2.100(2)		

distorted octahedral coordination geometry with four μ_1-bridged oxygen atoms from four independent squarate dianions and two hydroxyl groups (Figure 1a). Structural investigation

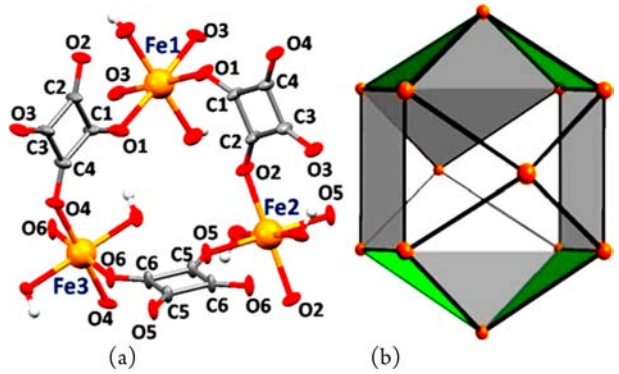

Figure 1. (a) View of the basic molecular unit of **1**. Color codes: saffron, Fe; gray, C; light gray, H; red, O. (b) Polyhedral view of the cuboctahedral nanoscopic cage of **1** after removing all atoms except Fe(II).

reveals a rarely observed polyhedral "cuboctahedron"[14] cage obtained by connecting only Fe(II) atoms through imaginary lines (Figure 1b). The cage has no internal crystallographic symmetry such that all Fe(II) ions are crystallographically independent. Thus, the three-dimensional framework (Figure 2) can also be viewed as an infinite array of densely packed cuboctahedral nanoscopic cages (Figure 3).

Further analysis of the structure shows a star-shaped arrangement (Figure 4a) of the 12 metal centers bridged by 4-fold monodentate squarate ligands, with prominent variation in bond angles (84.18(2)−93.21(2)°) around Fe(II) centers. The variation in the bond angles arise due to different degrees of inclination of the squarate ligands around the metal centers. The squarate ions in the framework exhibit parallel arrangements having distances of ∼8.18 Å between the planes. The noted longer distance is due to the intervention of μ_4-squarate ions in between, which form another array nearly perpendicular (86.78°) to the earlier parallel alignment. The Fe(II) ions in **1** are arranged in a 1D fashion through anti−anti $\mu_{1,3}$-O bridged single squarate ion along the b axis. The adjacent 1D chains are connected by $\mu_{1,2}$-O bridged squarate ions to form a 2D sheet. The 2D sheets are further connected through anti−anti $\mu_{1,3}$-O bridged squarate ions resulting in a 3D framework.

It is also noticed that the framework contains two types of voids. The smaller ones are hydrophilic as they have coordinated hydroxyl groups on the surface of the voids,

dx.doi.org/10.1021/ic401886f | Inorg. Chem. 2013, 52, 12064−12069

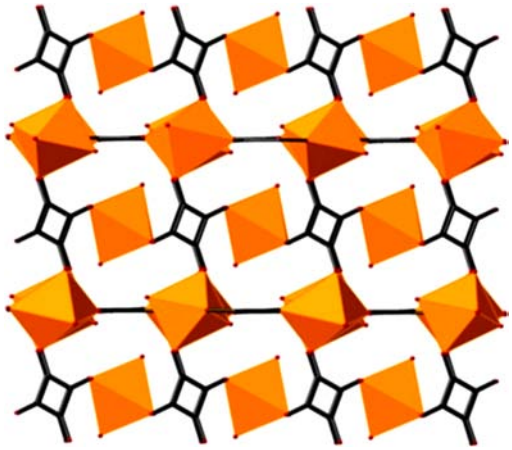

Figure 2. Polyhedral view of the 3D framework in **1** along *b* axis. Color codes same as in Figure 1

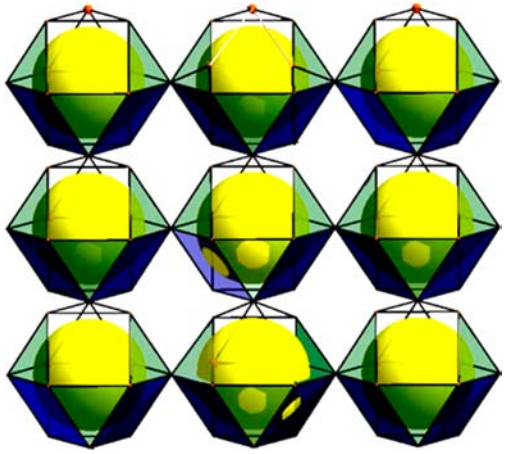

Figure 3. 3D framework formed by an infinite extension of cuboctahedral nanoscopic cages.

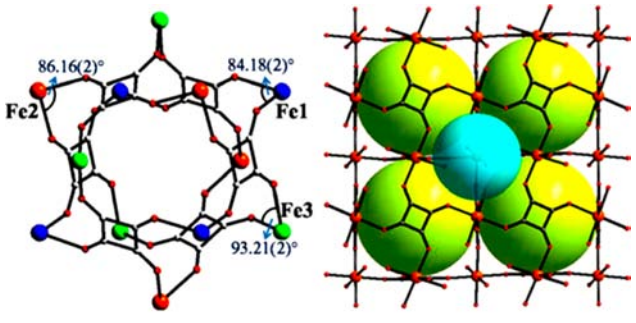

Figure 4. (a) Perspective view of the star-shaped core of complex **1**. Different colors for Fe(II) centers are used to differentiate them based on angles. (b) View of voids in the framework with van der Waals spheres (mean diameters 4.7 Å and 8.2 Å) inside.

while the aromatic squarate ligands form the surface of the larger voids, making them hydrophobic (Figure 4b). PLATON[15] analysis suggests only 18.8% (410.7 Å^3 out of the 2186.5 Å^3 per unit cell volume) pore accessible volume. Interestingly, both the voids, with estimated diameters of 4.7 Å (distance between two opposite hydroxyl groups) and 8.2 Å (Cg···Cg distance between two squarate ligands on the opposite faces of the cube), respectively, are empty but not accessible, as the opening to the voids are blocked by the squarate ligands. This is further confirmed by the gas adsorption study (Figure S5 and S6 in the Supporting Information). The coordinated hydroxyl groups on the surface of the smaller voids are connected by bifurcated hydrogen bonding interaction[16] (Table S1) with oxygen atoms of squarate ligands rendering further stability to the framework. In addition, the bridged squarato ligand is planar in nature. In comparison to the bond distances between Fe−O (squarate) bonds followed by the corresponding squarate C−O bonds, lengthening of the Fe(1)−O(3) (2.132(5)Å) bond was found, which results in a shorter C(3)−O(3) bond length (1.249(8) Å) with respect to rest of the C−O bonds. Similarly, lengthening of the Fe(2)−O(5) bond (2.128(4) Å) in comparison to the Fe(3)−O(6) bond (2.122(4) Å) provokes shortening of the C(5)−O(5) bond length in comparison to the C(6)−O(6) bond. The bond lengths around the C−O bonds are comparable to those reported for the free squaric acid and its lithium salts.[9−11] The mean values of C−C−C and O−C−C bond angles are 90.0(5)° and 134.98(6)°, respectively, very close to those reported for the nonchelating squarate.[9−11]

Spectroscopic and Thermogravimetric Characterization. The infrared spectrum of **1** (Figure S1) exhibits characteristic bands of the squarate moiety. The peak around 1521 cm^{-1} is in agreement with the existence of $C_4O_4^{2-}$ with roughly D_{4h} symmetry. This band is similar to that found in the spectrum of $K_2C_4O_4$, which has been assigned to a mixture of C−O and C−C stretching vibration modes.[17] Also the presence of the −OH group is confirmed from the spectra showing a prominent peak at 3433 cm^{-1}. The thermogravimetric profile of complex **1** has been measured to test the stability under air conditions. As shown in Figure S2, the weight loss of **1** from 130 to 170 °C is ∼17% (calcd. 16%), corresponding to the loss of two coordinated hydroxyl groups. Stability of the framework was observed up to ∼230 °C, after which it started decomposing.

Magnetic Property Studies. The purity of the as-synthesized product was indicated by the good agreement of the bulk phase powder X-ray diffraction patterns with the one simulated on the basis of the single crystal structure data (Figure S3). The powder was used for magnetic property measurements. The thermal variation of $\chi_M T$ (χ_M = molar magnetic susceptibility) of **1** is shown in Figure 5. At room temperature, a $\chi_M T$ value of 9.94 cm^3 K mol^{-1} is obtained, which is slightly higher than the spin-only value for three Fe(II) centers (9 cm^3 K mol^{-1}). This is due to the orbital contribution of the octahedral Fe(II) ion. On cooling, a smooth decrease in $\chi_M T$ proceeds until a minimum value of 6.65 cm^3 K mol^{-1} is reached at 7.5 K (T_{min}). Below T_{min}, $\chi_M T$ goes on a sharp rise up to 12.69 cm^3 K mol^{-1} at ∼5 K because of the ferromagnetic (FM) interactions between adjacent spins. At T < 5 K, $\chi_M T$ again experiences an abrupt drop, which appears to arise from antiferromagnetic (AFM) arrangements of spins within the framework. This is the signature of canted antiferromagnetic behavior (Scheme S2).[12] Above 7.5 K, the magnetic data nicely fit the Curie−Weiss equation [$\chi_M T = C/(T - \theta)$], affording a Curie constant C = 10.1 cm^3 K mol^{-1} and Weiss temperature θ = −6.1 K (Figure 5). The negative value of θ ensures AFM coupling among the neighboring spins with long-range Néel ordering below 7.5 K and also spin−orbit coupling effect.[18,19] In addition, bifurcation of FC (field-cooled) and ZFC (zero

dx.doi.org/10.1021/ic401886f | Inorg. Chem. 2013, 52, 12064−12069

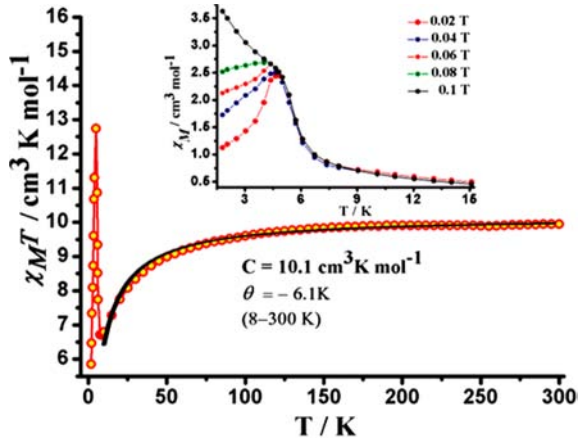

Figure 5. $\chi_M T$ vs T curve measured at 0.1 T. The black solid line shows the best fit to the Curie–Weiss equation. The inset curve presents the temperature dependence of the field-cooled magnetization (FCM) at various fields.

field-cooled) curves, measured at 0.06 T, is noticed below 5 K (Figure 6), which clearly indicates the ordering. The inset of

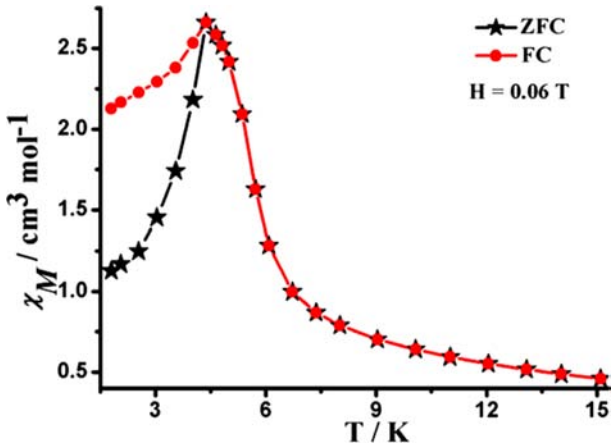

Figure 6. χ_M vs T plot measured at 0.06 T showing bifurcation of FC and ZFC curves below 5 K.

Figure 5 shows FC magnetization curves from 0.02 to 0.1 T, where peaks of χ_M are observed at ~5 K, up to 800 Oe, above which it disappears. From the inset of Figure 7, we also observe the intersection of the isothermal magnetization curves at the critical field of 800 Oe. The observed results clearly give us a hint of antiferromagnetic ordering or reorientation of domains in the lower temperature regime, which is most likely due to the field induced spin polarization.[20−22]

The field dependence of magnetization (Figure 7) shows a value of 6.67 NμB at 7 T per Fe3 unit, which is much below the saturation value of 12 NμB for three independent S = 2 spins with g = 2 but higher than the value of 4 NμB expected for three antiferromagnetically coupled Fe(II) ions. This intermediate value of the magnetization data can be elucidated as follows: AFM coupling takes place between the neighboring Fe(II) ions separated by a minimum distance of 5.84 Å (Scheme 1), but due to the pronounced spin−orbit coupling for the $^5T_2$ ground state of the Fe(II) in the octahedral environment, antisymmetric exchange is favored.[12] This results in a canting between the S_{Fe} = 2 local spins which would otherwise align antiparallel below 7.5 K (T_{min}).

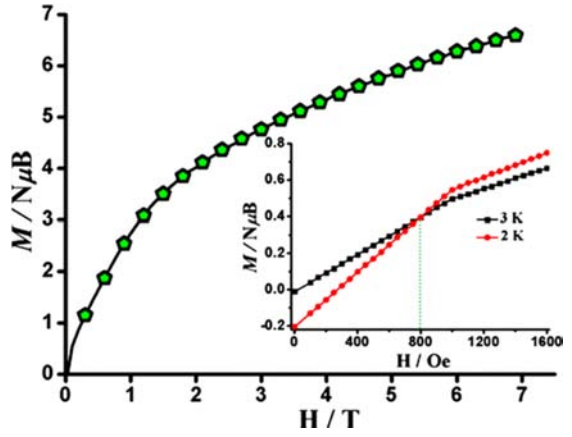

Figure 7. Field dependence of magnetization of **1** at 1.8 K. The inset plot shows intersection of the magnetization curves at 2 and 3 K at 800 Oe.

Scheme 1. Illustration of Planes Showing Different Distances between the Fe(II) Centers and the Dihedral Angle Affecting Spin Canting

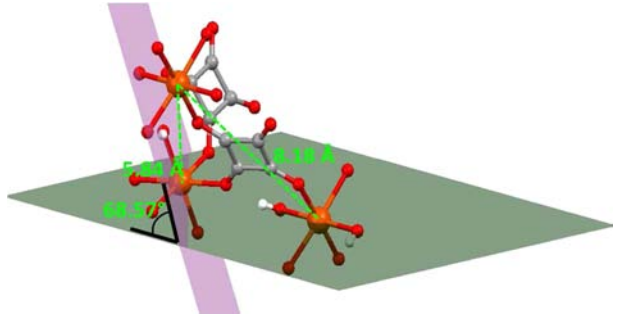

Additionally, a beautiful hysteresis loop is observed at 1.8 K with a coercive field of 680 Oe and a remnant magnetization M_R of 0.35 NμB (Figure 8). The canting angle α can be

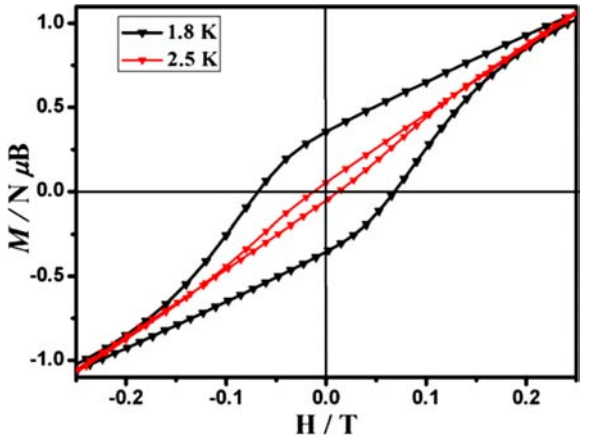

Figure 8. Hysteresis loop for **1** at 1.8 and 2.5 K.

estimated from the values of remnant magnetization (M_R) and saturation magnetization (M_S) by the equation $\sin(\alpha) = M_R/M_S$. We obtained a canting angle of 3.03° (M_S = 6.6 NμB (for three octahedral Fe(II) atoms of S_{eff} = 2 and g = 2.0). Two factors, single-ion magnetic anisotropy and antisymmetric exchange interaction, are primarily responsible for spin canting behavior in any molecule. The relatively large canting angle in

dx.doi.org/10.1021/ic401886f | Inorg. Chem. 2013, 52, 12064−12069

our case may be attributed to the presence of anisotropic Fe(II) ions and the antisymmetric exchange interaction in the anti−anti $\mu_{1,3}$ squarate-oxygen bridge between Fe(II) centers.

It is also important to note here that the Jahn−Teller (J−T) axis at an Fe(II) site is defined by the axial Fe−O bond direction, indicating the orientation of the single-ion magnetic anisotropy.[22] So, along the *b* axis, the spins are collinear and parallel to the J−T axis, while the adjacent ions have different orientations of the J−T axes with an angle of 68.57° between the axes (Scheme 1). Considering planes through the J−T axis, we can say that the presence of slanted basal planes of highly anisotropic Fe(II) ions is basically responsible for the spin-canting effect in the complex.

The ac magnetization dynamics were also investigated as a function of temperature (1.8−10 K) and frequency (ν = 1−782 Hz), in zero dc and a 3.5 Oe ac field. A sharp peak was observed at 5.2 K in both χ' and χ'' vs *T* plots (Figure 9 and S4), and no prominent frequency dependence was observed, confirming the long-range ordering of canted antiferromagnet.

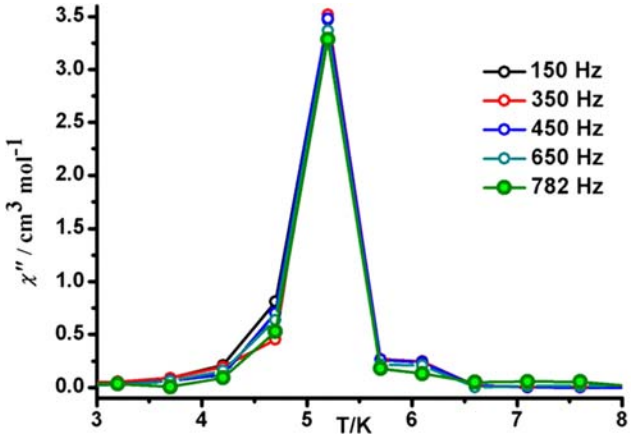

Figure 9. Out-of-phase AC magnetic susceptibility plot for complex **1**.

CONCLUSIONS

In summary, we have illustrated the design and synthesis of a three-dimensional MOF with squashed nanoscopic cuboctahedral cages. The aesthetically important structural feature in the complex is the presence of a "cuboctahedron," obtained by the array of 12 Fe(II) centers, containing six square and eight triangular faces around a substantial central cavity, which makes the overall three-dimensional framework an infinite extension of cuboctahedral nanoscopic cages. The gas uptake amounts do not gain prominence probably because of the role of squarate ligands as obstruction to the voids. But the material is elegant in the sense that it is the first squarate based system to exhibit dominant spin-canted antiferromagnetic behavior having long-range magnetic ordering at lower temperatures. This effort would open a new avenue for fabricating MOFs with more complex morphologies using simple ligands for different advanced applications.

ASSOCIATED CONTENT

Supporting Information

Includes schemes of different bridging modes of the squarate dianion with metal ions and spin canting; IR, TGA, PXRD, and magnetic plots; gas adsorption study; and hydrogen bonding table. This material is available free of charge via the Internet at http://pubs.acs.org. CCDC-931819 contains the supplementary crystallographic data for this paper. These data can be obtained free of charge from The Cambridge Crystallographic Data Center via www. ccdc.cam.ac.uk/data_request/cif.

AUTHOR INFORMATION

Corresponding Author

*E-mail: skonar@iiserb.ac.in. Fax: +91-755-4092392. Tel: +91-755-4092336.

Notes

The authors declare no competing financial interest.

ACKNOWLEDGMENTS

S.G. and S.B. acknowledge IISER Bhopal for the Ph.D. fellowships. A.A. thanks CSIR for an SRF fellowship. H.S.J. thanks IISER Bhopal for a postdoctoral fellowship. S.K. thanks DST, Government of India (Project No.SR/FT/CS-016/2010) and IISER Bhopal for generous financial and infrastructural support.

REFERENCES

(1) (a) Argent, S. P.; Adams, H.; Riis-Johannessen, T.; Jeffery, J. C.; Harding, L. P.; Ward, M. D. *J. Am. Chem. Soc.* **2006**, *128*, 72. (b) Al-Rasbi, N. K.; Tidmarsh, I. S.; Argent, S. P.; Adams, H.; Harding, L. P.; Ward, M. D. *J. Am. Chem. Soc.* **2008**, *130*, 11641. (c) Liu, Y.; Hu, C.; Comotti, A.; Ward, M. D. *Science* **2011**, *333*, 436. (d) Aoki, S.; Shiro, M.; Kimura, E. *Chem.—Eur. J.* **2002**, *8*, 929. (e) Olenyuk, B.; Whiteford, J. A.; Fechtenkötter, A.; Stang, P. J. *Nature* **1999**, *398*, 796.

(2) (a) Bunzen, J.; Iwasa, J.; Bonakdarzadeh, P.; Numata, E.; Rissanen, K.; Sato, S.; Fujita, M. *Angew. Chem., Int. Ed.* **2012**, *51*, 3161. (b) Li, D.; Zhou, W.; Landskron, K.; Sato, S.; Kiely, C. J.; Fujita, M.; Liu, T. *Angew. Chem., Int. Ed.* **2011**, *50*, 5182. (c) Osuga, T.; Murase, T.; Fujita, M. *Angew. Chem., Int. Ed.* **2012**, *51*, 12199. (d) Ning, G.−H.; Inokuma, Y.; Fujita, M. *Chem. Asian J.* **2013**, DOI: 10.1002/asia.201300758. (e) Suzuki, K.; Tominaga, M.; Kawano, M.; Fujita, M. *Chem. Commun.* **2009**, 1638. (f) Harris, K.; Fujita, D.; Fujita, M. *Chem. Commun.* **2013**, *49*, 6703. (g) Osuga, T.; Murase, T.; Ono, K.; Yamauchi, Y.; Fujita, M. *J. Am. Chem. Soc.* **2010**, *132*, 15553. (h) Fang, Y.; Murase, T.; Sato, S.; Fujita, M. *J. Am. Chem. Soc.* **2013**, *135*, 613. (i) Inokuma, Y.; Kawano, M.; Fujita, M. *Nature Chem.* **2011**, *3*, 349. (j) Sun, Q.-F.; Sato, S.; Fujita, M. *Nature Chem.* **2012**, *4*, 330. (k) Sun, Q.-F.; Iwasa, J.; Ogawa, D.; Ishido, Y.; Sato, S.; Ozeki, T.; Sei, Y.; Yamaguchi, K.; Fujita, M. *Science* **2010**, *328*, 1144.

(3) (a) Schoedel, A.; Cairns, A. J.; Belmabkhout, Y.; Wojtas, L.; Mohamed, M.; Zhang, Z.; Proserpio, D. M.; Eddaoudi, M.; Zaworotko, M. J. *Angew. Chem., Int. Ed.* **2013**, *52*, 2902. (b) Schoedel, A.; Wojtas, L.; Kelley, S. P.; Rogers, R. D.; Eddaoudi, M.; Zaworotko, M. J. *Angew. Chem., Int. Ed.* **2011**, *50*, 11421. (c) Subramanian, S.; Zaworotko, M. J. *Angew. Chem., Int. Ed.* **1995**, *34*, 2127. (d) Perry, J. J., IV; Perman, J. A.; Zaworotko, M. J. *Chem. Soc. Rev.* **2009**, *38*, 1400. (e) Moulton, B.; Zaworotko, M. J. *Chem. Rev.* **2001**, *101*, 1629. (f) Mohamed, M. H.; Elsaidi, S. K.; Wojtas, L.; Pham, T.; Forrest, K. A.; Tudor, B.; Space, B.; Zaworotko, M. J. *J. Am. Chem. Soc.* **2012**, *134*, 19556.

(4) (a) Fujita, M.; Tominaga, M.; Hori, A.; Therrien, B. *Acc. Chem. Res.* **2005**, *38*, 369. (b) Garay, A. L.; Pichon, A.; James, S. L. *Chem. Soc. Rev.* **2007**, *36*, 846. (c) Stang, P. J.; Seidel, S. R. *Acc. Chem. Res.* **2002**, *35*, 972. (d) Fiedler, D.; Leung, D. H.; Bergman, R. G.; Raymond, K. N. *Acc. Chem. Res.* **2005**, *38*, 349. (e) Koblenz, T. S.; Wassenaar, J.; Reek, J. N. H. *Chem. Soc. Rev.* **2008**, *37*, 247. (f) Bell, Z. R.; Harding, L. P.; Ward, M. D. *Chem. Commun.* **2003**, 2432.

(5) (a) McKinlay, A. C.; Morris, R. E.; Horcajada, P.; Férey, G.; Gref, R.; Couvreur, P.; Serre, C. *Angew. Chem., Int. Ed.* **2010**, *49*, 6260. (b) Boldog, I.; Gaspar, A. B.; Martínez, V.; Pardo-Ibñnez, P.; Ksenofontov, V.; Bhattacharjee, A.; Gütlich, P.; Real, J. A. *Angew. Chem., Int. Ed.* **2008**, *47*, 6433. (c) Rocca, J. D.; Liu, D.; Lin, W. *Acc. Chem. Res.* **2011**, *44*, 957. (d) Hazra, A.; Kanoo, P.; T. K. Maji, T. K.

Chem. Commun. **2011**, *47*, 538. (e) Murray, L. J.; Dinca, M.; Long, J. R. *Chem. Soc. Rev.* **2009**, *38*, 1294. (f) Maspoch, D.; Ruiz-Molina., D.; Veciana, J. *Chem. Soc. Rev.* **2007**, *36*, 770; *J. Mater. Chem.* **2004**, *14*, 2713. (g) Seo, J. S.; Whang, D.; Lee, H.; Jun, S. I.; Oh, J.; Jeon, Y. J.; Kim, K. *Nature* **2000**, *404*, 982. (h) Abrahams, B. F.; Hoskins, B. F.; Michail, D. M.; Robson, R. *Nature* **1994**, *369*, 727.

(6) Kurmoo, M. *Chem. Soc. Rev.* **2009**, *38*, 1353.

(7) (a) Kuppler, R. J.; Timmons, D. J.; Fang, Q.-R.; Li, J.-R.; Makal, T. A.; Young, M. D.; Yuan, D.; Zhao, D.; Zhuang, W.; Zhou, H.-C. *Coord. Chem. Rev.* **2009**, *253*, 3042. (b) Rao, C. N. R.; Cheetham, A. K.; Thirumurugan, A. *J. Phys.: Condens. Matter* **2008**, *20*, 083202.

(8) (a) Gatteschi, D.; Sessoli, R.; Villain, J. *Molecular Nanomagnets*; Oxford University Press: New York, 2006. (b) Miller, J. S. *Chem. Soc. Rev.* **2011**, *40*, 3266. (c) Beltran, L. M. C.; Long, J. R. *Acc. Chem. Res.* **2005**, *38*, 325. (d) Tasiopoulos, A. J.; Vinslava, A.; Wernsdorfer, W.; Abboud, K. A.; Christou, G. *Angew. Chem., Int. Ed.* **2004**, *43*, 2117.

(9) (a) Konar, S.; Corbella, M.; Zangrando, E.; Ribas, J.; Chaudhuri, N. R. *Chem. Commun.* **2003**, 1424. (b) Lloret, F.; Julve, M.; Faus, J.; Solans, X.; Journaux, Y.; Morgenstern-Badarau, I. *Inorg. Chem.* **1990**, *29*, 2232. (c) Long, G. J. *Inorg. Chem.* **1978**, *17*, 2702. (d) Trombe, J.-C.; Sabadie, L. P.; Millet, P. *Solid State Sci.* **2002**, *4*, 1209. (e) Kiskin, M. A.; Shvedenkov, Y. G.; Ikorskii, V. N.; Romanenko, G. V.; Ovcharenko, V. I. *Russ. Chem. Bull. Int. Ed.* **2003**, 52.

(10) (a) Kumagai, H.; Sobukawa, H.; Kurmoo, M. *J. Mater. Sci.* **2008**, *43*, 2123. (b) Greve, J.; Jeß, I.; Näther, C. *J. Solid State Chem.* **2003**, *175*, 328. (c) Carranza, J.; Sletten, J.; Lloret, F.; Julve, M. *Inorg. Chim. Acta* **2011**, *371*, 13.

(11) (a) Louka, F. R.; Stewart, A. D.; Regel, E.; Mautner, F. A.; Demeshko, S.; Meyer, F.; Massoud, S. S. *Inorg. Chem. Commun.* **2012**, *22*, 60. (b) Ghosh, A. K.; Ghoshal, D.; Zangrando, E.; Ribas, J.; Chaudhuri, N. R. *Dalton Trans.* **2006**, 1554. (c) Xanthopoulos, C. E.; Sigalas, M. P.; Katsoulos, G. A.; Tsipis, C. A.; Hadjikostas, C. C.; Terzis, A.; Mentzafo, M. *Inorg. Chem.* **1993**, *32*, 3743. (d) Akhriff, Y.; Server-Carrió, J.; Sancho, A.; García-Lozano, J.; Escrivá, E.; Soto, L. *Inorg. Chem.* **2001**, *40*, 6832. (e) Yufit, D. S.; Price, D. J.; Howard, J. A. K.; Gutschke, S. O. H.; Powell, A. K.; Wood, P. T. *Chem. Commun.* **1999**, 1561. (f) Solans, M.; Aguilb, A.; Gleizes, J.; Faus, M.; Julve, M.; Verdaguer, M. *Inorg. Chem.* **1990**, *29*, 775. (g) Alleyne, B. D.; Hall, L. A.; Hosein, H.-A.; Jaggernauth, H.; White, A. J. P.; Williams, D. J. *J. Chem. Soc., Dalton Trans.* **1998**, 3845. (h) Xanthopoulos, C. E.; Sigalas, M. P.; Katsoulos, G. A.; Tsipis, C. A.; Hadjikostas, C. C.; Terzis, A.; Mentzafos, M. *Inorg. Chem.* **1993**, *32*, 3743. (i) Jayaramulu, K.; Krishna, K. S.; George, S. J.; Eswaramoorthy, M.; Maji, T. K. *Chem. Commun.* **2013**, *49*, 3937. (j) Biswas, S.; Adhikary, A.; Goswami, S.; Konar, S. *Dalton Trans.* **2013**, *42*, 13331. (k) Goswami, S.; Adhikary, A.; Jena, H. S.; Konar, S. *Dalton Trans.* **2013**, *42*, 9813.

(12) Kahn, O. *Molecular Magnetism*; VCH Publishers Inc.: New York, 1991.

(13) (a) Sheldrick, G. M. *SHELXS-97*; University of Göttingen: Göttingen, Germany, 1997. (b) Sheldrick, G. M. *SHELXL-97*; University of Göttingen: Göttingen, Germany, 1997.

(14) (a) Williams, R. *The Geometrical Foundation of Natural Structure: A Source Book of Design*; Dover Publications: Mineola, NY, 1979; ISBN 0-486-23729-X (section 3-9). (b) Veblen, O.; Wesley Young, J. *Projective Geometry*; Ginn: Boston, MA, 1938.

(15) Spek, A. L. *J. Appl. Crystallogr.* **2003**, *36*, 7.

(16) (a) Alleyne, B. D.; Hall, L. A.; Hosein, H.-A.; Jaggernauth, H.; White, A. J. P.; Williams, D. J. *J. Chem. Soc., Dalton Trans.* **1998**, 3845.

(17) (a) Akhriff, Y.; Server-Carrió, J.; Sancho, A.; Garcia-Lozano, J.; Escrivá, E.; Soto, L. *Inorg. Chem.* **2001**, *40*, 6832. (b) Duggan, D. M.; Barefield, E. K.; Hendrickson, D. N. *Inorg. Chem.* **1973**, *12*, 985. (c) West, R.; Niu, H. J. *J. Am. Chem. Soc.* **1963**, *85*, 2589.

(18) Zeng, M.-H.; Zhou, Y.-L.; Wu, M.-C.; Sun, H.-L.; Du, M. *Inorg. Chem.* **2010**, *49*, 6436.

(19) Miller, J. S.; Drillon, M. *Magnetism: Molecule to Materials*; Wiley-VCH: Weinheim, Germany, 2005; pp 347.

(20) Yao, R.-X.; Qin, Y.-L.; Ji, F.; Zhao, Y.-F.; Zhang, X.-M. *Dalton Trans.* **2013**, *42*, 6611.

(21) Song, X.-J.; Muddassir, Md.; Chen, Y.; Wang, H.-S.; Song, Y.; You, X.-Z. *Dalton Trans.* **2013**, *42*, 1116.

(22) Zheng, Y.-Z.; Xue, W.; Tong, M.-L.; Chen, X.-M.; Grandjean, F.; Long, G. J. *Inorg. Chem.* **2008**, *47*, 4077.